

# An LQG Approach to the Control of Unmanned Wing-In-Ground Vehicle

Sofija Ilić

*Centro de Automática y Robótica (CAR) UPM-CSIC*  
*Universidad Politécnica de Madrid*  
Madrid, Spain  
0009-0002-3961-9946

Ramon A. Suarez Fernandez

*Centro de Automática y Robótica (CAR) UPM-CSIC*  
*Universidad Politécnica de Madrid*  
Madrid, Spain  
0000-0003-4102-5899

Zorana Milošević

*Centro de Automática y Robótica (CAR) UPM-CSIC*  
*Universidad Politécnica de Madrid*  
Madrid, Spain  
0000-0002-8701-5701

Claudio Rossi

*Centro de Automática y Robótica (CAR) UPM-CSIC*  
*Universidad Politécnica de Madrid*  
Madrid, Spain  
0000-0002-8740-2453

Sergio Domínguez

*Centro de Automática y Robótica (CAR) UPM-CSIC*  
*Universidad Politécnica de Madrid*  
Madrid, Spain  
0000-0002-9498-5407

**Abstract**—In this paper, we propose a Linear Quadratic Gaussian (LQG) approach to control an unmanned Wing-In-Ground (WIG) vehicle. We use a nonlinear and nonstationary state-space six degrees of freedom (6 DOF) model, obtained by system identification, around the trimmed operating point. Implementing the proposed control strategy includes defining the desired trajectory of motion, linearizing the model around the trim operating point, and computing adequate controller gains. The feasibility of implementing the proposed approach has been demonstrated through system behavior simulations in various conditions using Matlab and Simulink.

**Index Terms**—WIG vehicle, control system, LQG, mathematical model, ground effect

## I. INTRODUCTION

Numerous works on nonlinear systems control for various kinds of vehicles can be found in the literature, such as [1] where feedback control for flight control systems is presented, [2] in which stabilizing back-stepping controller for moored and free-floating ships is designed, the comparison of two non-linear model-based control strategies for autonomous cars analyzed in [3] and back-stepping control and nonlinear optimization for position and attitude control of hybrid drones described in [4]. However, when looking into the solutions to the WIG vehicle control problem, the body of literature narrows down significantly. Some of the research papers deal with this problem in the way of applying linear or nonlinear control strategies to complete nonlinear models described with coupled and time-varying equations such as [5] and [6]. On

the other hand, there are papers approaching this problem by decoupling linearized models and focusing on controlling longitudinal or lateral dynamics, such as [7], [8] and [9], or [10]. One can also find a handful of comparative analysis review papers such as [11] which compares stability and safety characteristics of control strategies with and without feedback and useful advice and strategies for control implementation, such as described in [12].

WIG vehicles use the ground effect, which reduces the drag force and increases the lift force. Due to this, WIG vehicles can fly at low altitudes and high speeds and achieve high energy efficiency while carrying heavy loads. Despite the century-long study of WIG vehicles, controlling WIG vehicles remains a significant challenge. Advances in computing and control strategies now offer the potential to solve these control issues, ensuring safe and efficient operation across different flight regimes. The subject of this paper is the design of a WIG vehicle control system using the LQG control strategy. The LQG strategy can be applied to a wide range of multivariable nonlinear and non-stationary systems and is a combination of already known control concepts - Linear Quadratic (LQ) control and the Kalman filter. This strategy assumes that the state-space model of the system is known and is often applied to systems with multiple input and output variables.

The remainder of the paper is laid out as follows. In Section I, the introduction is presented, including the literature review of the stated challenge. Section II is dedicated to the mathematical modeling of the system, which includes defining reference frames, state and control vectors, and forces and torques acting on the vehicle, resulting in a final system of

This work was supported by the AIRSHIP project of the Horizon Europe Framework Programme (Grant Agreement No. 101096487).

equations of WIG vehicle motion. Section III introduces the LQG strategy, trimming the WIG vehicle model using numerical optimization and model linearization around the operating trim point. The simulation results, performance evaluation, and conclusion are given in Section IV and Section V, respectively.

## II. MATHEMATICAL MODEL

A mathematical model is fundamental in science and engineering, as it is a very useful and compact way to capture known knowledge about a process. In general, it is not possible to form an entire model based only on knowledge of physical laws, but some parameters are determined by experimental methods. The biggest challenge in mathematical system modeling is determining the state variables, which essentially describe the dynamics of flow and storage of energy and mass in the system, so positions and velocities are most often used as states. The proposed system modeling principle draws inspiration from various models found in the literature. One of them is the Research Civil Aircraft Model [13] which is a twin-engine civil aircraft model developed by the Group for Aeronautical Research and Technology in Europe. For mathematical modeling, this craft is viewed as a rigid body, with possible translation and rotation around the  $x$ -,  $y$ - and  $z$ -axis, which is transferable to the mathematical modeling of WIG vehicles. In this section, the necessary concepts of mathematical modeling of the WIG vehicle are presented and described in detail, equations of motion are derived and analyzed, and the necessary notation is established. More precisely, in the following subsections, reference frames, state vector and control surfaces, forces, and moments acting on the WIG vehicle are defined and a mathematical model in the state space is presented.

### A. Reference Frames

To describe the dynamics of the WIG vehicle, including the forces and moments that act on it, we must first define the reference frames. In the literature, the standard reference frame used to describe the dynamic equations of a 6 DOF system are the following:

- North-East-Down (NED) Reference Frame - Inertial reference frame, whose axes are located as shown in Fig. 1, the  $x$ -axis is pointing north, the  $y$ -axis is pointing east, and the  $z$ -axis pointing toward the center of the Earth.
- Reference frame fixed to the body - The reference frame whose origin is fixed to the center of gravity of the vehicle. Its axes are located as shown in Fig. 1,  $x_B$  is pointing in the direction of the vehicle nose,  $y_B$  is pointing to the right wing and  $z_B$  is pointing downward.
- Wind Reference Frame - It is used to describe aerodynamic forces in the form of dimensionless coefficients. The  $x_V$ -axis is aligned with the velocity vector that is obtained after rotating the  $y_B$ -axis according to the angle of attack and the  $x_B$ -axis according to the side-slip angle, as shown in Fig. 1.

### B. System of Equations of Motion

The motion of the WIG vehicle can be described by standard nonlinear differential equations of motion, with possible translation and rotation about  $x$ ,  $y$ , and  $z$  axes, known as the 6 DOF model [14] in the following form:

$$\begin{aligned} m(\dot{v}_B + \omega \times v_B) &= F_m \\ J\dot{\omega} + \omega \times J\omega &= M_m \\ \dot{x}_i &= T_{ob}v_B \\ \dot{\Phi} &= R\omega \end{aligned} \quad (1)$$

where the vector  $\Phi$  represents the Euler angles vector,  $\omega$  is vector of angular velocities,  $v_B$  represents the velocity vector relative to the body reference frame,  $x_i$  represents the velocity vector relative to the NED reference frame,  $R$  is the rotation matrix,  $T_{ob}$  is the translation matrix,  $m$  is mass of the vehicle and  $F_m$  and  $M_m$  represent the force and moment vectors acting on the WIG vehicle. To derive the mathematical model of the WIG vehicle in the presented form, it is necessary to adopt certain assumptions:

- 1) WIG vehicle is considered as a rigid body;
- 2) The mass of the WIG vehicle is constant in time;
- 3) The Earth is considered a flat ground and at the same time an inertial reference frame.

With the adopted assumptions, it is possible to apply first and second Newton's laws of motion. The external forces acting on the WIG vehicle are considered a combination of gravitational, aerodynamic, and propulsion forces

$$F = F_g + F_a + F_{t1} + F_{t2} \quad (2)$$

and the external moments are a combination of aerodynamic and propulsion moments

$$M = M_a + M_{t1} + M_{t2} \quad (3)$$

For expressing aerodynamic forces and moments in the wind reference frame, which is aligned with the direction of the wind, aerodynamic coefficients  $C_D, C_Q, C_L, C_l, C_m, C_n$ , and the following aerodynamic angles were introduced:

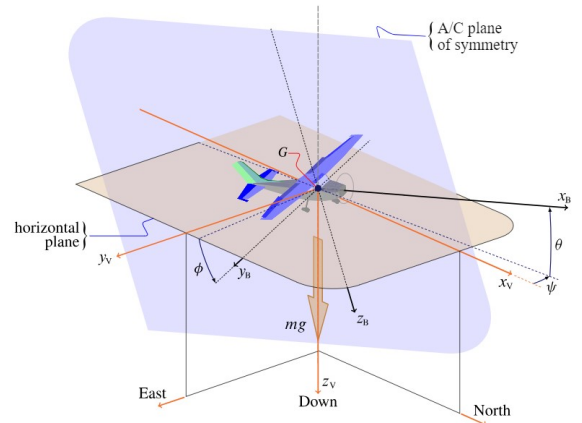


Fig. 1. Reference Frames

- Angle of attack  $\alpha$  - Angle formed by the direction of the longitudinal axis of the body with the  $x$  component of the velocity vector of the body  $u$  and is defined as  $\alpha = \arctan\left(\frac{w}{u}\right)$ .
- Side-slip angle  $\beta$  - Angle formed by the direction of the longitudinal axis of the body with the  $y$  component of the velocity vector of the body  $v$ . It is defined as  $\beta = \arcsin\left(\frac{v}{V_a}\right)$ .
- Air-mass-referenced flight path angle  $\gamma_a$  - Angle formed by the velocity of the center of mass of the vehicle. When negative, the plane descends and vice versa, and it plays a fundamental role in defining level flight conditions. It is defined as  $\gamma_a = \theta - \alpha$ .

The state vector consists of variables that describe the state of the WIG vehicle, which are linear velocities  $u, v, w$ , Euler angles  $\phi, \theta, \psi$ , angular velocities  $p, q, r$  and position in NED reference frame  $x_c, y_c, z_c$ , in vector form as

$$x = [u, v, w, \phi, \theta, \psi, p, q, r, x_c, y_c, z_c]^T \quad (4)$$

The control vector reflects the control surfaces of the WIG vehicle, in this particular case elevator, ailerons, rudder, and two throttles, respectively in vector form

$$U = [\delta_e, \delta_a, \delta_r, \delta_{t1}, \delta_{t2}]^T \quad (5)$$

where  $\delta_e$  is elevator deflection,  $\delta_a$  aileron deflection,  $\delta_r$  rudder deflection,  $\delta_{t1}$  and  $\delta_{t2}$  are  $[0, 100]$  percentage signals of the total achievable exerted engine force. It is assumed that the wind speed  $V_w$  and side-slip angle  $\beta$  are equal to zero, therefore following simplifications are considered:

- Airspeed is equal to ground speed  $V_a = V_g$
- Velocity is equal to velocity relative to the air mass  
 $u = u_r, v = v_r$  and  $w = w_r$
- Heading angle equals course angle  $\psi = \chi$
- Flight path angle equals air-mass-referenced flight path angle  $\gamma = \gamma_a$

Taking into account previously adopted reference frames and analyzed forces and moments, the equations of motion in the state space are:

$$\dot{u} = -\frac{1}{2}\rho V_a^2 \frac{S}{m} (C_D \cos \alpha \cos \beta + C_Q \cos \alpha \sin \beta - C_L \sin \alpha) + \frac{F_{t1} + F_{t2}}{m} - g \sin \theta - qw + rv \quad (6)$$

$$\dot{v} = -\frac{1}{2}\rho V_a^2 \frac{S}{m} (C_D \sin \beta - C_Q \cos \beta) + g \sin \phi \cos \theta - ru + pw \quad (7)$$

$$\dot{w} = -\frac{1}{2}\rho V_a^2 \frac{S}{m} (C_D \sin \alpha \cos \beta + C_Q \sin \alpha \sin \beta + C_L \cos \alpha) + q \cos \theta \cos \phi - pv + qu \quad (8)$$

$$\dot{p} = \frac{C_l \frac{1}{2}\rho V_a^2 S}{J_{xx}} \quad (9)$$

$$\dot{q} = \frac{C_m \frac{1}{2}\rho V_a^2 S + (J_{zz} - J_{xx})}{J_{yy}} \quad (10)$$

$$\dot{r} = \frac{C_n \frac{1}{2}\rho V_a^2 S + (J_{xx} - J_{yy})qp}{J_{zz}} \quad (11)$$

$$\dot{\psi} = \frac{r \cos \phi + q \sin \phi}{\cos \theta} \quad (12)$$

$$\dot{\phi} = p + (r \cos \phi + q \sin \phi) \tan \theta \quad (13)$$

$$\dot{\theta} = q \cos \phi - r \sin \phi \quad (14)$$

$$\dot{X}_c = R \cdot [u, v, w]^T \quad (15)$$

where  $C_D, C_Q, C_L, C_l, C_m, C_n$  are aerodynamic coefficients,  $\frac{1}{2}\rho V_a^2 S$  air pressure, with  $\rho, S$  and  $m$  being air density, wing area and total mass of the vehicle,

$\dot{X}_c = [x_c, y_c, z_c]^T$ ,  $J = \begin{bmatrix} J_{xx} & J_{xy} & J_{xz} \\ J_{yx} & J_{yy} & J_{yz} \\ J_{zx} & J_{zy} & J_{zz} \end{bmatrix}$  inertia matrix

and  $R = \begin{bmatrix} c\theta c\psi & c\psi s\theta s\phi - s\psi c\phi & s\phi s\psi + s\theta c\psi c\phi \\ c\theta s\psi & s\psi s\theta s\phi + c\psi c\phi & s\theta s\psi c\phi - s\phi c\psi \\ -s\theta & s\phi c\theta & c\phi c\theta \end{bmatrix}$  where  $c$  and  $s$  represent cos and sin of the respective Euler angles.

### III. LQG CONTROL STRATEGY

LQG strategy is an approach in control theory that belongs to linear control techniques that optimize quadratic functions. It combines two well-known and most-used concepts in control theory: the LQ approach and the Kalman filter. The LQ concept aims to find the optimal control law that minimizes the quadratic cost function, considering system states and control signals. The implementation of this strategy assumes knowledge of system dynamics and noise-free measurements. The Kalman filter estimates the system's state by combining measurements with noise and knowledge of the system's dynamics. It provides an optimal state estimation, even in the presence of noise in the measurements. Therefore, the LQG controller ensures a stable and robust system response to disturbances and noise, and it is widely used for controlling Multiple Input and Multiple Output (MIMO) systems. Before applying the LQG control strategy technique, it is necessary to select operating points and linearize the model around them. Then, based on the linearized model, the LQG controller is designed. The LQG control technique aims to minimize the following criterion function

$$J = \int_0^\infty (x(t)^T Q x(t) + u(t)^T R u(t)) dt \quad (16)$$

by generating the control signal

$$u(t) = -K(t)x(t) \quad (17)$$

where  $Q$  and  $R$  are weighting matrices,  $K(t)$  gain which is calculated from the following equation

$$K(t) = -R(t)^{-1} B(t)^T S(t) \quad (18)$$

in which  $S(t)$  is the solution to the Riccati differential equation. The first step in designing an LQG controller is to calculate the LQ optimal gain. For the calculation of the optimal gain, it is necessary to adopt appropriate weighting

matrices that significantly affect the controller performance. There are certain empirical recommendations for adopting the initial values of the weight matrices. Then, the optimal values are determined by observing the system's behavior for the adopted parameters. For the observed system, the weight matrices were determined using the trial-and-error method, starting from the recommended values until matrix values that achieved satisfactory results were found. Based on the weight matrices, by solving the Riccati equation, the corresponding LQ gains were calculated, and then the Kalman filter was designed for the estimation of all variable states. It is important to note that as input variables of the Kalman filter, correction control signals and obtained deviations of the output variables from the nominal values are passed on, and then the estimated deviations of the state variables are multiplied by the LQ gain and added to the nominal control signal. The control system with an incorporated LQG controller that generates the corrective control signal is presented in the following block scheme in Fig. 2, where the plant block represents the behavior of the system when the trim control values are applied.

#### A. Trimming the WIG Vehicle

Adopting the operating working point is a necessary step for linearizing the nonlinear equations describing the system dynamics and the subsequent application of the LQG controller. For aerial navigation, the operating points are usually chosen as longitudinal equilibrium states in which the velocity and gravity vectors lie in the plane of symmetry of the vehicle, i.e., operating points that correspond to flight modes such as steady flight, climbing, or descending. Since the principle of flying a WIG vehicle is based on the maximum use of the ground effect in steady flight, it is desirable to ensure a steady flight at a certain speed without a change in direction. In steady flight, the WIG vehicle balances out forces in two directions. Vertically, the lift force matches the gravity force so the vehicle neither rises nor falls. Horizontally, the thrust force equals the drag force so the vehicle moves at a constant speed. This balance ensures a smooth and stable flight. Also, in steady flight, there is no change in the starting values of the state variables, therefore it is valid that the first derivatives of the nine state variables are equal to zero. The objective was to compute trim states and inputs when the WIG vehicle

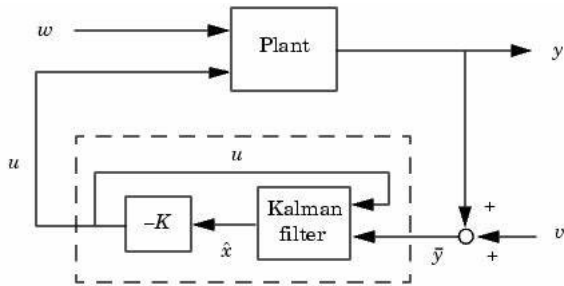


Fig. 2. LQG Block Scheme

is in cruise steady-state flight, simultaneously satisfying the following conditions:

- Travelling at constant trimmed steady-state flight speed  $V_a^* = 85m/s$
- Constant flight path angle  $\gamma$  equal to zero
- Constant speed  $\dot{u}^* = \dot{v}^* = \dot{w}^* = 0$
- Constant roll and pitch angles  $\dot{\phi}^* = \dot{\theta}^* = \dot{p}^* = \dot{q}^* = 0$

The control and state values, which ensure the presented trim condition, were calculated using numerical optimization, considering the limitations of the control signals. By minimizing the criterion function  $J_2 = P^T W P$ , where  $P$  is a vector of previously introduced trim conditions and  $W$  is the weighted identity matrix, the following trim values of control signals, states, and their first derivatives for applied trim control values were obtained using the Nelder-Mead simplex search method [15]

$$u^* = [0, -0.178, 0, 0.0821, 0.0821]^T \quad (19)$$

$$x^* = [84.9905, 0, 1.2713, 0, 0, 0, 0, 0, 0.0150, 0]^T \quad (20)$$

$$\dot{x}^* = [0]_{9 \times 1} \quad (21)$$

#### B. Linearization around operating trim point

Model linearization around the previously chosen operating trim point was performed using the small perturbation theory. Because the functions in the state space system model around the chosen operating point are time-invariant, they can be represented with first-order Taylor expansion. The resulting linearized model is given in matrix form as

$$\frac{d\Delta x(t)}{dt} = A\Delta x(t) + B\Delta u^*(t) \quad (22)$$

$$\Delta y(t) = H\Delta x(t) + D\Delta u^*(t) \quad (23)$$

where  $H = I_{9 \times 9}$ ,  $D = [0]_{9 \times 9}$ ,  $\Delta u^*(t) = \begin{bmatrix} \Delta u(t) \\ 1 \end{bmatrix}$ .

As a final step, the controllability, observability, and stability of the linearized system were analyzed using Kalman's tests and plotting the pole-zero graph. The outcome of the analysis was that the system is controllable and observable and possesses marginal stability, which was expected due to unstable WIG vehicle dynamics.

## IV. SIMULATION RESULTS AND DISCUSSION

After the model and controller were implemented in the chosen software Matlab and Simulink, measurement noise and disturbance were modeled and used for robustness analysis of system behavior. The behavior of the system was simulated for 1000 seconds with different Gaussian white noise present in the measured state signals and disturbance applied to the state  $u$  during the time interval  $[700, 750]s$  with amplitude 50% of the trim value of the state. The simulation results of the closed-loop system with the LQG controller and the Kalman filter with the conditions presented are shown in the following Fig. 3 to Fig. 9. Furthermore, to analyze compliance with the conditions previously introduced for steady-state flight, Table I shows squared errors for the most important variables.

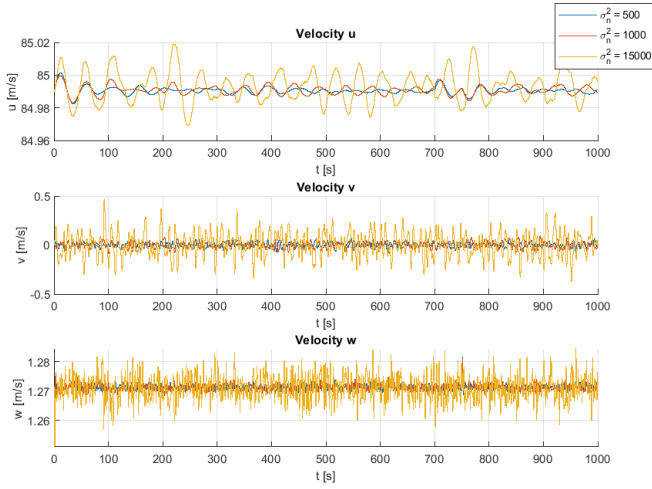


Fig. 3. Linear Velocities

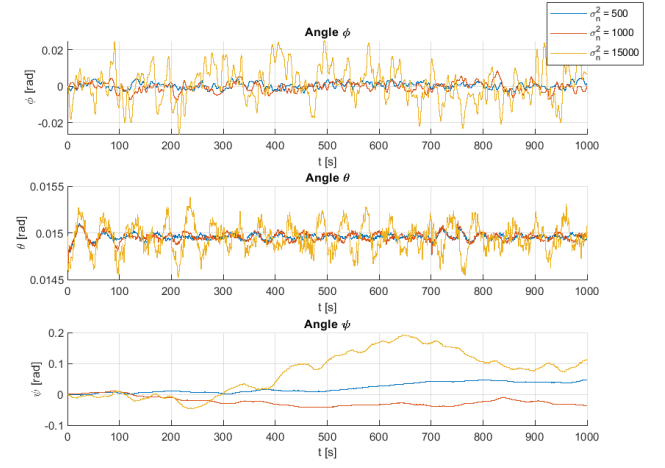


Fig. 5. Euler Angles

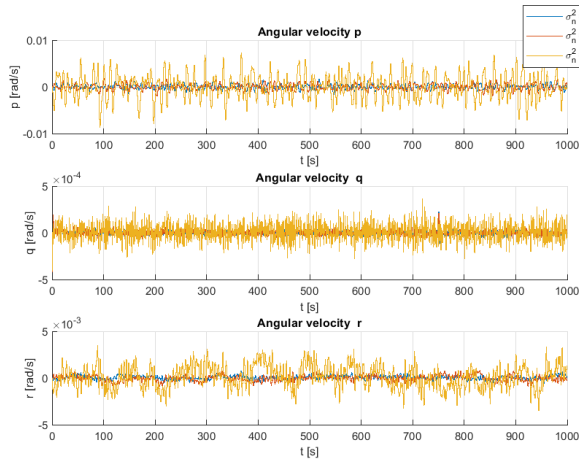


Fig. 4. Angular Velocities

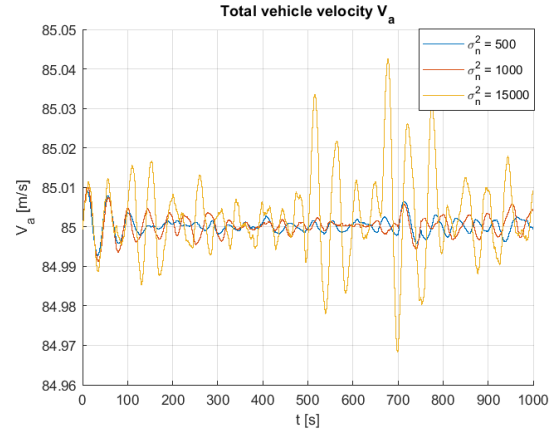


Fig. 6. Total Vehicle Velocity

From the graphs shown, we can notice that as the noise level increases, deviations from the nominal values and oscillations follow the same trend and are visible in all state variables. Nevertheless, these deviations are very small-scale, and the controller manages to cope with this disturbance. Looking at the behavior during the interval of action of the disturbance in the state variable  $u$ , we can notice greater peaks present in the total velocity  $V_a$ , especially at the moment of activating and deactivating the disturbance. Furthermore, the maximum amplitude of the total velocity increases with the increase of the noise level; still, the deviations from the nominal signal are insignificant, in the value range of approximately  $10^{-5}$  to  $10^{-3}$ , with respect to the increase in the noise level, as shown in Table I. Altogether, increasing noise levels leads to consistent oscillations across all state variables, although these remain minor, and the controller effectively mitigates them. During disturbance presence in the state variable  $u$ , notable peaks occur in total velocity  $V_a$ , with peak amplitudes increasing alongside noise levels, yet the controller preserves

insignificant deviations from the nominal signal.

## V. CONCLUSIONS AND FUTURE WORK

This paper analyzes the possibility of implementing LQG control as a cost-effective strategy to control an unmanned WIG vehicle. The performance of the proposed approach has been demonstrated through its application to the control of the

TABLE I  
MEAN SQUARED ERROR FOR DIFFERENT NOISE LEVELS

$\sigma_n^2$	500	1000	15000
$MSE_{V_a}$	$9.900110^{-5}$	0.0001061	0.00016868
$MSE_{\gamma}$	0.00022369	0.0002237	0.00022355
$MSE_{\dot{u}}$	$9.44110^{-8}$	$1.485210^{-7}$	$2.304810^{-6}$
$MSE_{\dot{v}}$	0.00027449	0.00051591	0.0074713
$MSE_{\dot{w}}$	$2.653810^{-6}$	$4.126410^{-6}$	$4.032310^{-5}$
$MSE_{\dot{\phi}}$	$2.344810^{-7}$	$4.570810^{-7}$	$7.368410^{-6}$
$MSE_{\dot{\theta}}$	$4.487810^{-10}$	$6.946610^{-10}$	$6.784410^{-9}$
$MSE_{\dot{p}}$	$1.032810^{-7}$	$1.939110^{-7}$	$2.861110^{-6}$
$MSE_{\dot{q}}$	$2.664910^{-9}$	$4.492810^{-9}$	$5.028210^{-8}$

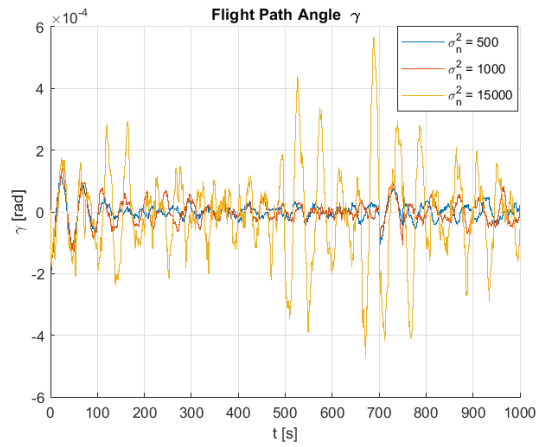


Fig. 7. Flight Path Angle

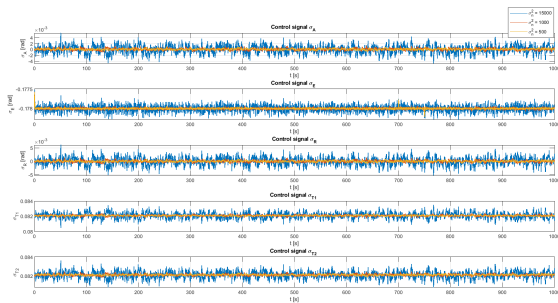


Fig. 8. Control Signals

WIG vehicle around the chosen trim operating point reflecting steady-state flight. Furthermore, the practical robustness of the proposed controller was analyzed through simulations in the presence of measurement noise and disturbance in one of the state variables. Presented results have shown that the LQG controller serves as an efficient and robust tool for accomplishing trim condition state of nonlinear and nonstationary system dynamics with cost-efficiency in various conditions, including the presence of system disturbance and measurement noise. This approach represents the initial step toward controlling unmanned WIG vehicles. In the future, algorithms for calculating and adapting cost and noise ma-

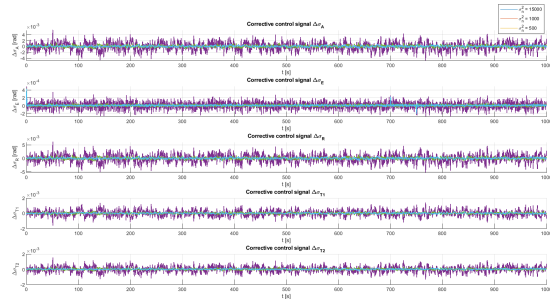


Fig. 9. Corrective Control Signals

trices can be used to improve controlled system performance. Likewise, the possibility of implementing a sequential LQG approach proposed in [16] to follow a predefined trajectory that includes take-off and landing will be analyzed. Future work includes exploring the possibilities of implementing nonlinear and adaptive techniques and analyzing system behavior with designed controllers, accompanying the implementation of the control system to physical prototypes, and performing adequate field tests to analyze the full system behavior.

## REFERENCES

- [1] J. Hauser, S. Sastry, and G. Meyer, "Nonlinear controller design for flight control systems\*," IFAC Proceedings Volumes, vol. 22, no. 3, pp. 385–390, 1989. Nonlinear Control Systems Design, Capri, Italy, 14-16 June 1989.
- [2] J. Peter Strand, K. Ezal, T. I. Fossen, and P. V. Kokotović, "Nonlinear control of ships: A locally optimal design," IFAC Proceedings Volumes, vol. 31, no. 17, pp. 705–710, 1998. 4th IFAC Symposium on Nonlinear Control Systems Design 1998 (NOLCOS'98), Enschede, The Netherlands, 1-3 July.
- [3] E. Alcalá, L. Sellart, V. Puig, J. Quevedo, J. Saludes, D. Vázquez, and A. Lopez, Comparison of two non-linear model-based control strategies for autonomous vehicles, p. 846–851. Institute of Electrical and Electronics Engineers (IEEE), 2016.
- [4] G. Serrano, B. J. Guerreiro, and R. Cunha, "Nonlinear control of hybrid drones via optimised control allocation," in CONTROL 2022 (L. Brito Palma, R. Neves-Silva, and L. Gomes, eds.), (Cham), pp. 214–226, Springer International Publishing, 2022.
- [5] D. Patria, C. Rossi, R. A. S. Fernandez, and S. Dominguez, "Nonlinear control strategies for an autonomous wing-in-ground-effect vehicle," Sensors, vol. 21, no. 12, 2021.
- [6] Y. Pan, N. Li, W. Zou, B. Wang, K. Wang, X. Tang, S. Bu, and L. Qin, "An augmented sliding mode control for fixed-wing uavs with external disturbances and model uncertainties," Drones, vol. 7, no. 7, 2023.
- [7] A. Saeed, S. U. Ali, and M. Z. Shah, "Linear control techniques application and comparison for a research uav altitude control," in 2016 13th International Bhurban Conference on Applied Sciences and Technology (IBCAST), pp. 126–133, 2016.
- [8] Ingabire, Aline and Sklyarov, Andrey A., "Control of longitudinal flight dynamics of a fixedwing uav using lqr, lqg and nonlinear control," E3S Web Conf., vol. 104, p. 02001, 2019.
- [9] A. Nebylov, A. Panferov, and S. Brodsky, "Mathematical model and control system of an ekranoplan under the action of large aerodynamic loads," in 2021 IEEE 8th International Workshop on Metrology for AeroSpace (MetroAeroSpace), pp. 516–520, 2021.
- [10] A. Elkhatem and S. Engin, "Robust lqr and lqr-pi control strategies based on adaptive weighting matrix selection for a uav position and attitude tracking control," Alexandria Engineering Journal, vol. 61, 12 2021.
- [11] A. Groß, N. Kornev, T. Hahn, B. Lampe, and W. Drewelow, "Flight stability and safety of wig craft with and without feedback control," ASME 2014 12th Biennial Conference on Engineering Systems Design and Analysis, ESDA 2014, vol. 1, 07 2014.
- [12] A. Panferov, A. Nebylov, and S. Brodsky, "Features of designing control systems for wig-craft," in 2019 IEEE 5th International Workshop on Metrology for AeroSpace (MetroAeroSpace), pp. 136–141, 2019. Rome, Italy
- [13] D. Moormann, A. Varga, G. Looye, and G. Gr ubel, "Robustness analysis applied to autopilot design, part 3: Physical modeling of aircraft for automated lft generation applied to the research civil aircraft model," in Proc. of 21st Congress of the International Council of Aeronautical Sciences, 1998. LIDO-Berichtsjahr=1999,.
- [14] D. A. Caughey, "Introduction to aircraft stability and control course notes for m&ae 5070," 2011.
- [15] J. C. Lagarias, J. A. Reeds, M. H. Wright, and P. E. Wright, "Convergence properties of the nelder-mead simplex method in low dimensions," SIAM Journal on Optimization, vol. 9, no. 1, pp. 112– 147, 1998.
- [16] Z. M. Djurovic and B. D. Kovacevic, "A sequential lqg approach to nonlinear tracking problem," Intern. J. Syst. Sci., vol. 39, p. 371–382, april 2008